Boundary integral modelling of elastic wave propagation in multi-layered 2D media with irregular interfaces

E. Liu[1], Z.J. Zhang[2], J.-H. Yue[3] and A. Dobson[1]

[1]*British Geological Survey, West Mains Road, Edinburgh EH9 3LA, Scotland, UK*

[2]*Chinese Academy of Sciences, Being, China.*

[3]*Dept. of Geophy., China University of Mining & Technology, Xuzhou, 221008, China*

ABSTRACT

We present a semi-analytic method based on the propagation matrix formulation of indirect boundary element method to compute response of elastic (and acoustic) waves in multi-layered media with irregular interfaces. The method works recursively starting from the top-most free surface at which a stress-free boundary condition is applied, and the displacement-stress boundary conditions are then subsequently applied at each interface. The basic idea behind this method is the matrix formulation of the propagation matrix (PM) or more recently the reflectivity method as wide used in the geophysics community for the computation of synthetic seismograms in stratified media. The reflected and transmitted wave-fields between arbitrary shapes of layers can be computed using the indirect boundary element method (BEM, sometimes called IBEM). Like any standard BEM, the primary task of the BEM-based propagation matrix method (thereafter called PM-BEM) is the evaluation of element boundary integral of the Green's function, for which there are standard method that can be adapted. In addition, effective absorbing boundary conditions as used in the finite difference numerical method is adapted in our implementation to suppress the spurious arrivals from the artificial boundaries due to limited model space. To our knowledge, such implementation has not appeared in the literature. We present several examples in this paper to demonstrate the effectiveness of this proposed PM-BEM for modelling elastic waves in media with complex structure.

INSTRUCTION

Computation of elastic wave propagation in layered media with arbitrary shapes of interfaces has found applications in many areas, such as engineering, geophysics,

underwater acoustics, etc. Traditionally, domain-based finite difference or finite element methods are used. For stratified flat layered media, the propagation matrix or more recently reflectivity method can be used (Fuchs and Muller, 1971). Chen (1990, 1995, 1996) has extended the propagation matrix method to multi-layered media with irregular interfaces using the so-called global generalized reflection/transmission formulations. Recently the indirect Boundary Element Method (BEM) has been extended to model wave propagation in multi-layered media with arbitrary interfaces (see for examples, Bouchon et al., 1989; Bouchon & Coutant, 1994; Pedersen et al., 1996, Vai et al., 1999, and cited references in those papers). Note that BEM has been extensively used to study topographic effects using exact Green functions by Sanchez-Sesma and his co-authors (e.g. Sanchez-Sesma and Campillo, 1991). This method has a distinct advantage over domain-based methods in that only boundaries, or in the case of multi-layers interfaces, need to be discretized. This method is based on the matrix formulation of propagation matrix method (Fuchs and Muller, 1971; Kennett, 1981) and essentially works recursively to match boundary conditions at each successive interface (Pedersen et al., 1996). Reflection and transmission at internal interfaces are computed using the BEM. We shall refer to this method as PM-BEM. We have tested extensively the validity and limitations of the PM-BEM and its stability in a variety of situations, examining in particular dependence on source frequency, distance of the source from boundaries and separation of two boundaries. Comparison with results from the reflectivity method shows that this PM-BEM is very accurate. The method can be potentially used to perform large scale seismic modelling.

INDIRECT BOUNDARY ELEMENT METHOD

For simplicity, we shall consider 2D here. In the absence of body forces the displacement $\vec{u}$ at any point $\vec{x}$ in an area *V* surrounded by the boundary *S* (Figure 1) can be expressed as follow, i.e. mathematical description of Huygen's principle (Liu et al. 1997; Liu & Zhang, 2001; Pointer et al., 1998):

$$u_i(\vec{x}) = \int_S \varphi_j(\vec{x}')G_{ij}(\vec{x},\vec{x}')dS', \qquad (1)$$

where $\vec{G}_{ij}(\vec{x},\vec{x}')$ is the *i*th displacement Green's function at $\vec{x}$ due to a point source in *j*th direction at $\vec{x}'$ (the variable with an arrow above implies vector, matrix or tensor). $\varphi_j(\vec{x}')$ is the force density at $\vec{x}'$ in *j*th direction.

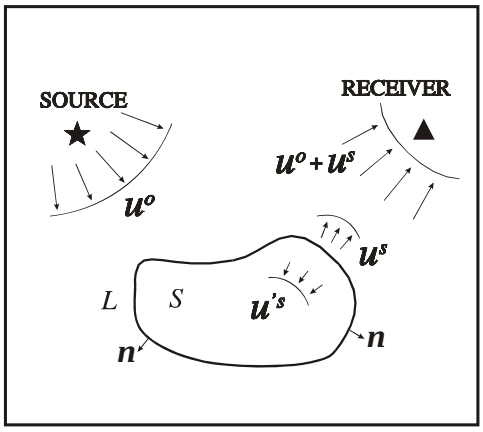

Figure 1. A scattering object *S* bounded by the curve *L* with outwards normal ***n***. Upon an incidence of $\boldsymbol{u}^0$ located at source the total wave-field received at receiver is the superposition of the incident wave-field $\boldsymbol{u}^0$ and the scattered wave-field $\boldsymbol{u}^s$.

The corresponding expression for traction, for a smooth boundary, is given by:

$$\tau_i(\vec{x}) = c\varphi_i(\vec{x}) + \int_S \varphi_j(\vec{x}')T_{ij}(\vec{x},\vec{x}')dS', \qquad (2)$$

where *c* is 0 if $\vec{x}$ is outside *S*, *c* is 0.5 if $\vec{x}$ tends to *S* from the inside *V*, and *c* is -0.5 if $\vec{x}$ tends to *S* from the outside *V* (Pointer al., 1998). $\tau_i(\vec{x})$ is the *i*th component traction on *S* at $\vec{x}$ and T_{ij} is the traction Green's function. The BEM based on equations (1) and (2) is known as the indirect BEM (Liu & Zhang, 2001; Pointer et al., 1998).

The total wave field u_i^{total} at receiver point $\vec{x}$ is the superposition of the direct wave u_i^0 from the source (called free field) and the scattered waves u_i^s, i.e.

$$u_i^{total} = u_i^0 + u_i^s. \qquad (3)$$

If we discretize the boundary *S* into *N* elements and combine equations (1) and (2) with (3) we obtain the following expressions for displacement and traction:

$$u_i(\vec{x}) = u_i^0(\vec{x}) + \sum_{n=1}^{N} \varphi_j(\vec{x}_n^{'}) \overline{G}_{ij}(\vec{x}, x_n^{'}), \tag{4}$$

where

$$\overline{G}_{ij}(\vec{x}, \vec{x}_n^{'}) = \int_{\Delta S_n} G_{ij}(\vec{x}, \vec{x}_n{}') dS', \tag{5}$$

and

$$\tau_i(\vec{x}) = c\,\tau_i^0(\vec{x}) + \sum_{n=1}^{N} \varphi_j(\vec{x}_n^{'}) \overline{T}_{ij}(\vec{x}, x_n^{'}), \tag{6}$$

where

$$\overline{T}_{ij}(\vec{x}, \vec{x}_n) = \frac{1}{2}\delta_{ij}\delta_{nk} + \int_{\Delta S_n} T_{ij}(\vec{x}, \vec{x}_n^{'}) dS'. \tag{7}$$

ΔS_n is the length of the *n*th element. If the surface forces densities $\vec{\varphi}$ are known then displacements and tractions can be computed for any source.

THE PROPAGATION MATRIX METHOD

We consider a model with of *M*+1 interfaces (refer to Figure 2 for the model configuration). Layers are numbered *m*=0 to *m*=*M*+1, where layer 0 is the free surface and layer *M*+1 is the last interface. *N* is the number of boundary points on each layer. We define the following four displacement-traction matrices $\vec{A}_{m,1}$, $\vec{A}_{m,2}$, $\vec{B}_{m,1}$ and $\vec{B}_{m,2}$ of the form (Pedersen et al., 1996):

$$\vec{A} = \begin{bmatrix} \mathfrak{I} \\ \mathfrak{R} \end{bmatrix}, \tag{8}$$

where

$$\mathfrak{I} = \begin{bmatrix} g_{11} & g_{13} \\ g_{31} & g_{33} \end{bmatrix} \quad \text{and} \quad \mathfrak{R} = \begin{bmatrix} t_{11} & t_{13} \\ t_{31} & t_{33} \end{bmatrix}$$

.

g_{ij} and t_{ij} are *N* x *N* matrices containing the *i*th components of the displacement and traction Green's functions from the *j*th component of the source. $\vec{A}_{1,m}$ contains the

Green's functions for receivers on interface *m* from sources on interface *m*. $\vec{A}_{2,m}$ contains the Green's functions for receivers on interface *m* from sources on interface *m-1*. $\vec{B}_{1,m}$ contains the Green's functions for receivers on interface *m-1* from sources on interface *m*. $\vec{B}_{2,m}$ contains the Green's functions for receivers on interface *m-1* from sources on interface *m-1*. $\vec{Q}_m$, a 4*N* vector, contains secondary sources for every segment on interface *m*, including the two components of the secondary sources. $\vec{Q}_m$ can be split into two vectors $\vec{Q}_{1,m}$ and $\vec{Q}_{2,m}$: $\vec{Q}_{1,m}$ being the secondary sources heading downwards into the layer from interface *m* and $\vec{Q}_{2,m}$ the secondary sources heading upwards into the layer from interface *m*. $\vec{F}_{1,m}$ is the free-field at interface *m* from the layer above. $\vec{F}_{2,m}$ is the free-field at interface *m* from the layer below.

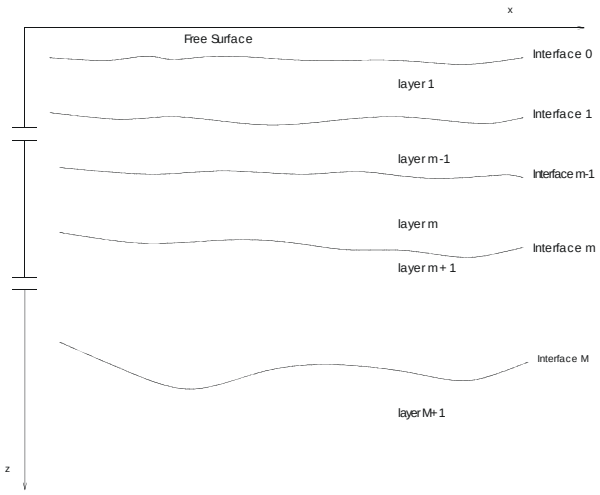

Figure 2. A multilayered model configuration.

Continuities of displacement and traction on the *m*th interface give us the following recursive relation:

$$\vec{A}_{m,2}\vec{Q}^T_{m-1,2} + \vec{A}_{m,1}\vec{Q}^T_{m,1} + \vec{F}^T_{m,1} = \vec{B}_{m+1,2}\vec{Q}^T_{m,2} + \vec{B}_{m+1,1}Q^T_{m+1} + \vec{F}^T_{m,2}. \quad (9)$$

We can write this equation in the form:

$$\vec{A}_{m,2}\vec{Q}^T_{m-1,2} = \vec{D}_m\vec{Q}^T_m + \vec{E}^T_m, \quad (10)$$

where $\vec{D}_M$ and $\vec{E}_M$ are defined as follows:

$$\vec{D}_m = [-\vec{A}_{m,1}; \vec{B}_{m+1,2} + \vec{B}^T_{m+1,1}(\vec{D}^{-1}_{m+1})^{\sup} \vec{A}_{m+1,2}], \quad (11)$$

$$E^T_m = -\vec{B}_{m+1,1}[(\vec{D}^{-1}_{m+1})^{\sup} \vec{E}^T_{m+1} + \Delta\vec{F}^T_m]. \quad (12)$$

For the deepest interface ($m = M+1$) these expressions become:

$$\vec{D}_m = [-\vec{A}_{M,1}; \vec{B}_{M+1,2}], \quad (13)$$

and

$$E^T_m = \Delta\vec{F}^T_M .]. \quad (14)$$

If $\vec{D}_M$ and $\vec{E}_M$ are computed and propagated upwards using equations (11) and (12) $\vec{D}_m$ and $\vec{E}_m$ matrices can be found for any layer. At interface m=0 (the free surface) the traction is equal to zero, we can obtain the following equation:

$$\vec{C}\vec{X}^T = \vec{Y}^T, \quad (15)$$

where

$$\vec{C} = \begin{bmatrix} -\vec{D}^{left}_1 & -\vec{D}^{right}_1 & \vec{A}_{1,2} \\ \vec{B}^{\inf}_{1,1} & 0 & \vec{B}^{\inf}_{1,2} \end{bmatrix}, \quad (16)$$

$$\vec{X} = \left[\vec{Q}_{1,1}; \vec{Q}_{1,2}; \vec{Q}_{0,2}\right] \quad (17)$$

and

$$\vec{Y} = \left[\vec{E}_1; -\vec{F}^{\inf}_{0,2}\right]. \quad (18)$$

Solving equation (16) yields the force distributions $\vec{Q}_{0,2}$, $\vec{Q}_{1,1}$ and $\vec{Q}_{1,2}$. We can then compute the force distributions for every interface working from top to bottom using equation (10). The displacement at any point $\vec{x}$ within the mth layer can be found by convolving the Green's function with the appropriate force distribution. The contribution to the displacement is found in this way for all the boundary points lying on the interfaces above and below layer *m*, and all the contributions are summed to give the displacement. In the case where the source and the receiver lie in the same layer the displacement from the incident wave should be added.

The coefficient matrix of the linear equations (equation 15) is a fully populated complex matrix and is non-symmetric. This is often regarded as the disadvantage of

BEM in comparison with finite element methods. Nevertheless, this matrix can be easily manipulated as the number of elements is not exceedingly high and the system of equations is only solved once for each frequency. A standard method such as the Gaussian elimination or *LU* decomposition can be used, and for large *M*, a conjugate gradient method can be used. In this paper we only use a standard *LU* decomposition method to solve the linear equations. The maximum number of elements is restricted by the power of current computers and it also depends on the specified accuracy. In general, the number of elements depends on the particular frequency considered. At low frequencies, a minimum number of elements is required, while at high frequencies this number should be chosen such that at least three surface elements are sampled per seismic wavelength to give satisfactory results (Bouchon & Coutant, 1994).

ABSORBING BOUNDARY CONDITIONS

Spurious waves will be generated from the edges of the models as a result of the truncation of layers. A simple way of reducing this effect is by introducing an absorbing zone at the edges of the models. We weight the Green's functions by an exponential function for segments within the absorbing zone (Cerjan et al., 1985).

$$w = \begin{cases} \exp\{-[a(W-x)]^2\}, & x < L \\ \exp\{-[(a(L-W+x)]^2\}, & x > x_{\max} - L \end{cases} \tag{19}$$

In other words, the displacements generated by the secondary sources in the absorbing zones are weighted by the above function to reduce its contributions to the overall displacements outside the absorbing zones. This is very similar to the application of Cerjan's et al. (1985) method for conventional finite difference methods (e.g. Vlastos et al. 2003). The variables *a* and *W* are the absorption factor and the absorption zone width respectively. *L* is the model size. *a*=0.001 is suggested. $x_{\max}$ is the model size (i.e. the maximum horizontal distance of our 2D models concerned). This simple technique was first proposed for FD method, and our tests show it can also be effectively used for PM-BEM.

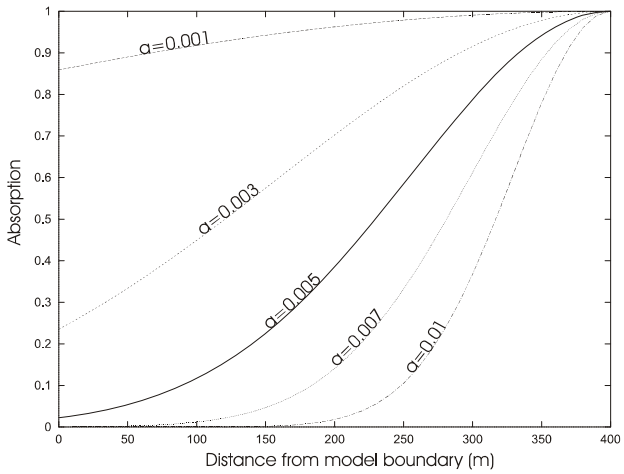

Figure 3. Variations of absorbing weight *w* with the distance from the model area/space for different parameter *a*.

Figure 3 shows the variation of absorbing function *w* with the distance from the boundary (of the model area or space) for different variations of parameter *a*. As we can see that the choice of parameter *a* is crucial for the effective elimination of the boundary effects. If *a* is too large, the absorbing area can be chosen to be small, but this will cause additional spurious reflections; if *a* is too small, a large absorbing area has to be used to allow the boundary reflection to arrive much later (as the reflected wave amplitudes are only slightly reduced).

IMPLEMENTATION AND NUMERICAL EXAMPLES

We implement our method in the frequency, that means that the frequency-domain displacements are computed for a range of frequencies (for the examples below, we typically consider the frequency ranges up to 200 Hz). The inverse FFT is then performed to calculate the time-domain response. Like any BEM cited in the Introduction, the memory requirements to store the layer matrices are quite large depending on the number of discretization needed for each layers. The basic requirement is that at least 3 elements are required for the minimum frequency used (see Sanchez-Sesma and Campilo, 1991). To speak up the computation, we divide the computational domain into 3 equal areas and then match the boundary conditions (continuity of stress and displacements) between each domain – this is called the domain decomposition (see Dobson et al., 2003). The adapt of the domain

decomposition is effectively reduce the size of layer matrices (used in equations 8-18) to one-third so that matrix inversions can be performed much fast.

Here we shall present two examples. We first consider a simple model containing only the flat free surface. This simple model is used to demonstrate the accuracy of the proposed PM-BEM. The source is located at a distance of *D* from the free surface. The receiver is fixed at 600m from the free surface and is immediately below the source (i.e. no horizontal offsets). We compare the vertical components of synthetic seismograms from PM-BEM presented in this paper using a vertical force source and results from the reflectivity method (Kennett, 1981). The results are shown in Figures 4 and 5 for different source depths and different frequencies. We see that there is a very good agreement between the two results except when the source is too close to the free surface (Figure 4), in which condition, very fine discretization grids, i.e. at least less than one-third of the distance between source and the free-surface, has to be used. This is understandable as the in our implementation of the PM-BEM, we only use the far-field Green's function and the near field terms have been ignored (same to the implementation of BEM by other authors cited in the Introduction).

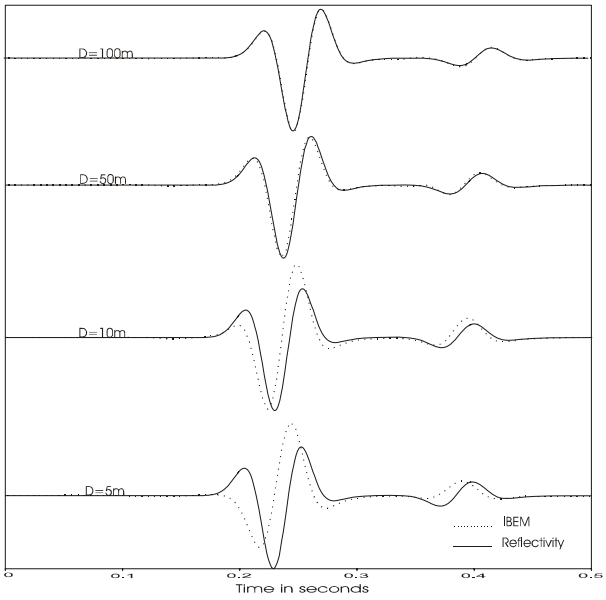

Figure 4. Comparison of synthetic seismograms for different source depths.

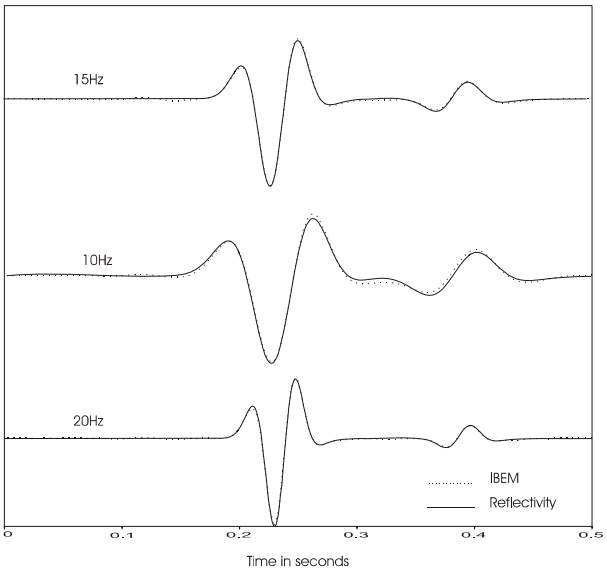

Figure 5. Comparison of synthetic seismograms for different frequencies.

Figure 6 shows a three-layer model. The top interface is a rough interface generated with a sine function (sine function has a period is 100m and the height of 10m). The parameters for each layer are given in the table next to Figure 6. The explosive source is located at the origin with a range of receivers along the flat free surfaces. We use a Ricker wavelet with a dominant frequency of 50Hz which gives the wavelengths of 66m for P-waves and 38m for shear-waves (using the velocities for the first layer). The horizontal and vertical synthetic seismograms are shown in Figure 7. We can clearly identify reflections from the top and lower interfaces. The reflection from the top sine interface shows periodical amplitude variations, while the reflection from the lower interface shows almost continuous variations. In general the amplitude variations will depend on the interface roughness (period and height of the sine in our case) and the wavelength. Our studies have revealed some interesting features, such as the interference patterns resulting in the periodical loss or enhancements of amplitudes as in light scattering - this feature is known as the localization of lights, and in our case, localization of seismic waves [see more discussion about the coherent backscattering or localization of seismic waves in Schultz and Toksoz, 1994; Larose et al., 2004).

CONCLUSIONS

We have presented results of modelling elastic wave propagation using the indirect BEM for layered media. This method uses the idea from the propagation matrix formulation and computes recursively the secondary source distributions at each interface. The BEM is very accurate as long as certain factors are taken into consideration. An absorbing boundary condition, developed for FD method, can be applied to effectively eliminate spurious waves due to interface truncations. The PM-BEM has a potential to be used as a tool to perform large scale seismic modelling, using, for example, the domain decomposition method (Dobson et al., 2003; Ziolkowski et al. 2003).

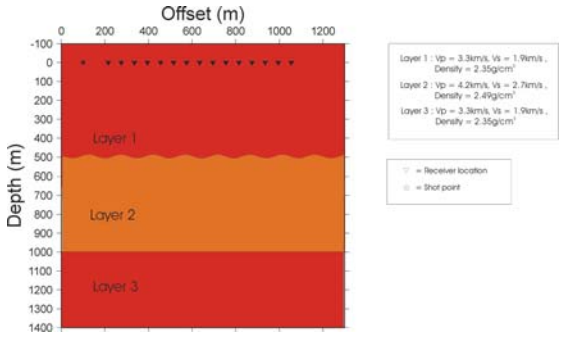

Figure 6. A three-layer model consisting a rough interface (modeled using a sine function). The parameters for each layer are shown in the table on the right side.

ACKNOWLEDGEMENTS

This work was carried out while the first author was on leave at CUMT (China), funded by the National Natural Science Foundation of China (40574056, 40564058). We thank the Editor Dr Lianjie Huang, reviewer Professor Francisco Sanchez-Sesma and another anonymous reviewer for very positive and constructive comments (and for additional references) that lead to the significant improvements of the readability of this paper. This paper is published with the permission of the Executive Director of the British Geological Survey (NERC).

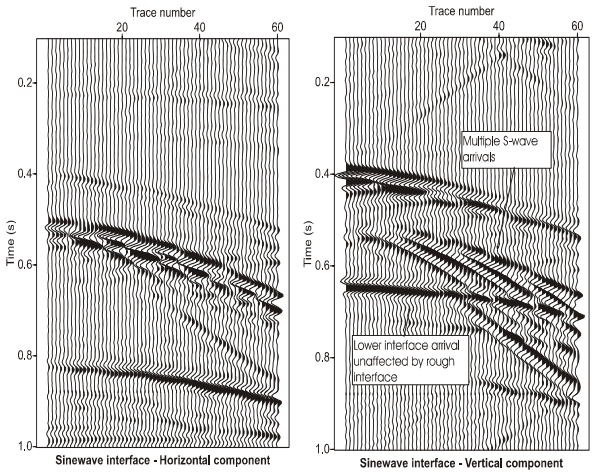

Figure 7. Horizontal and vertical synthetic seismograms corresponding to the model geometry shown in Figure 6.

REFERENCES

Bouchon, M., Campillo, M. & Graffet, S. 1989. A boundary integral equation-discrete wavenumber representation method to study wave propagation in multilayered media having irregular interface. *Geophysics* 54**:** 1134-1140.

Bouchon, M. & Coutant, O. 1994. Calculation of synthetic seismograms in a laterally varying medium by the boundary element-discrete wavenumber method. *Bull. Seis. Soc. Am.* 84**:** 1869-1881.

Cerjan, C., Kosloff, D., Kosloff, R. & Reshel, M. 1985. A nonreflecting boundary condition for discrete acoustic-wave and elastic-wave equations. Geophysics 50**:** 705-708.

Chen, X., 1990, Seismograms synthesis for multi-layered media with irregular interfaces by global generalized reflection/transmission matrices method. Part I. Theory of 2-D SH case, *Bull. Seism. Soc. Am*. 80: 1696-1724.

Chen, X., 1995, Seismograms synthesis for multi-layered media with irregular interfaces by global generalized reflection/transmission matrices method. Part II. Applications of 2-D SH case, Bull. Seism. Soc. Am. 85: 1094-1106.

Chen, X., 1996, Seismograms synthesis for multi-layered media with irregular interfaces by global generalized reflection/transmission matrices method. Part III. Theory of 2-D P-SV case", Bull. Seism. Soc. Am. 86: 389-405.

Dobson, A., Ritchie, D., Liu, E., Li, X.Y. & Ziolkowski, A. 2003. Modelling long-offset seismic waves for sub-basalt imaging. *73rd Ann. Int. SEG Meeting, Expanded Abstract, Dallas, Oct. 2003.*

Kennett, B.L.N. 1981. *Seismic wave propagation in stratified media*: Cambridge University Press.

Liu, E., Crampin, S. and Hudson, J.A., 1997. Diffraction of seismic wave by cracks with application to hydraulic fracturing: *Geophysics*, 62, 253-265

Liu, E. & Zhang, Z.J. 2001. Numerical study of elastic wave scattering by distributed cracks or cavities using the boundary integral method. *J. Comput. Acoust.* 9 (3): 1039-1054.

Larose, E., Margerin, L., van Tiggelen, B.A. & Campillo, M., 2004, Weak localisation of seismic waves, Phys. Rev. Lett., 93: 048501-1 – 048501-4.

Pedersen, H.A., Maupin, V. & Campillo, M., 1996, Wave diffraction in multilayered media with the indirect Boundary Element Method: application to 3-D diffractionof long-period surface waves by 2-D lithospheric structures. *Geophys. J. Int.* 125: 545-558.

Pointer, T., Liu, E. & Hudson, J.A. 1998. Numerical modelling of seismic waves scattered by hydrofractures: application of the indirect boundary element method. *Geophys. J. Int.* 135**:** 289-303.

Fuchs, K. & Muller, G., 1971, Computation of synthetic seismograms with the reflectivity method and comparison of observations, *Geophys. J. R. Astr. Soc*., 23: 417-433.

Sanchez-Sesma, F. J., & Campillo, 1991, M. Diffraction of P, SV and Rayleigh waves by topographic features: a boundary integral formulation, Bull. Seism. Soc. Am. 81: 2234–2253.

Schultz, C.A. and Toksoz, M.N, 1994, Enhanced backscattering of seismic waves from a highly irregular random interface: P-SV case: J. Geophy. Res., 117: 783-810.

Vai R, J. M. Castillo-Covarrubias, F. J. Sanchez-Sesma, D Komatistsch, & J.-P-Vilotte, 1999, Elastic wave propagation in an irregularly layered medium, *Soil Dynamics & Earthquake Engineering*, 18: 11-18.

Vlastos, S., Liu, E., Main, I.G. & Li, X.Y., 2003, Numerical simulation of wave propagation in media with discrete distributions of fractures: effects of fracture sizes and spatial distributions, Geophys. J. Int. 152: 649-668.

Ziolkowski, A., Gatliff, R., Li, X.Y., Hanssen, P., Jakubowicz, H., Hampson, G., Dobson, A. & Liu, E., 2003, Use of low frequencies for sub-basalt imaging, Geophys. Prosp. 51: 169-182.